(a)

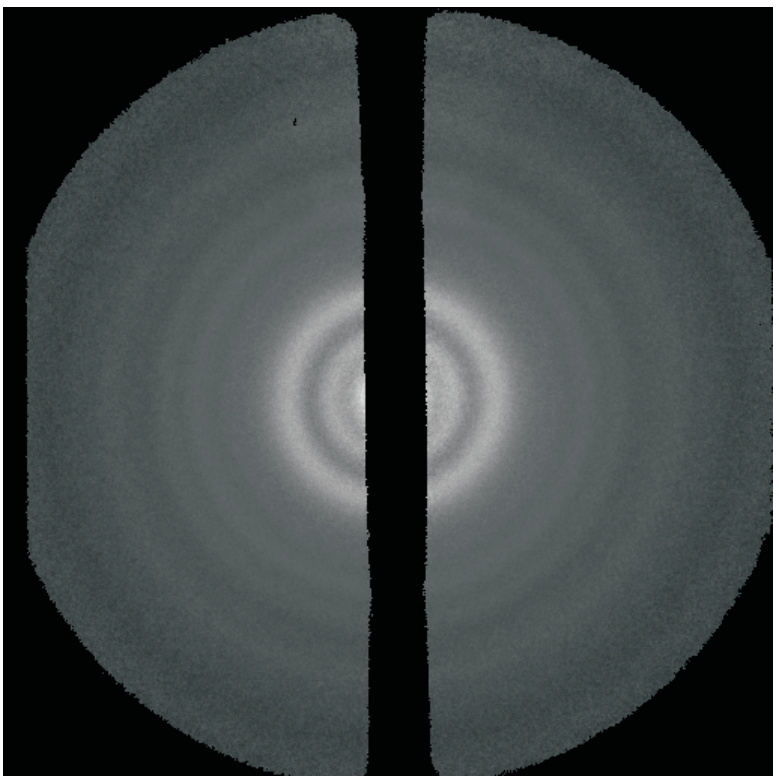

(b)

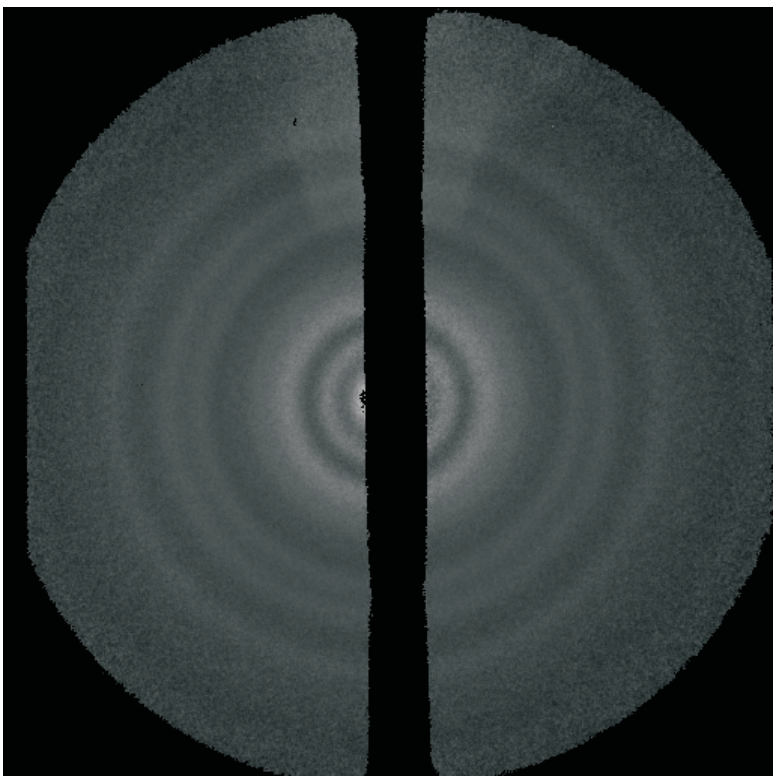

Fig. 5-1. The ratio patterns from diffraction by (a) chlorobenzene and (b) bromobenzene.

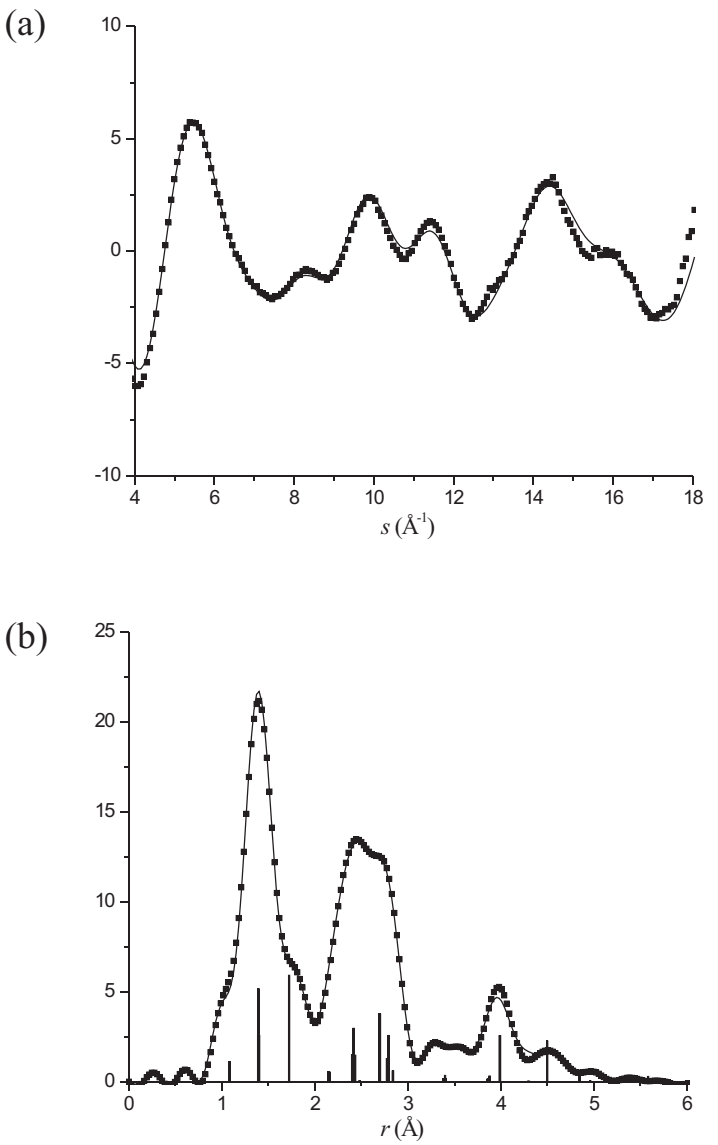

Fig. 5-2. The final refined theory (line) with experimental data (filled squares) for chlorobenzene in (a) $sM(s)$ and (b) $f(r)$ representations. The fitted theory is quantified with ^{2} = 233.021 and R = 0.110. The vertical bars at each peak position have a height proportional to nZ_iZ_j/r.

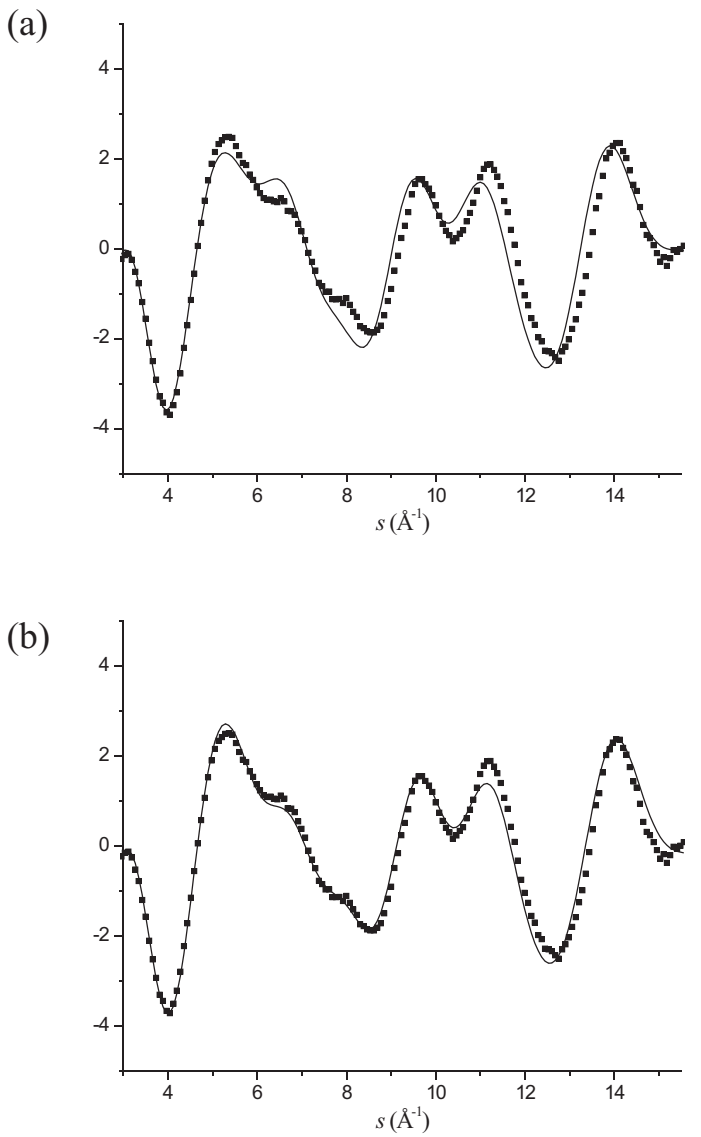

Fig. 5-3. $sM(s)$ curves for bromobenzene showing theory (line) with experimental data (filled squares). The theoretical curve in (a) corresponds to that derived from the DFT structure (^{2} = 1137.568; R = 0.241) and that in (b) is the DFT structure with a refined C–Br bond distance (^{2} = 201.465; R = 0.104).

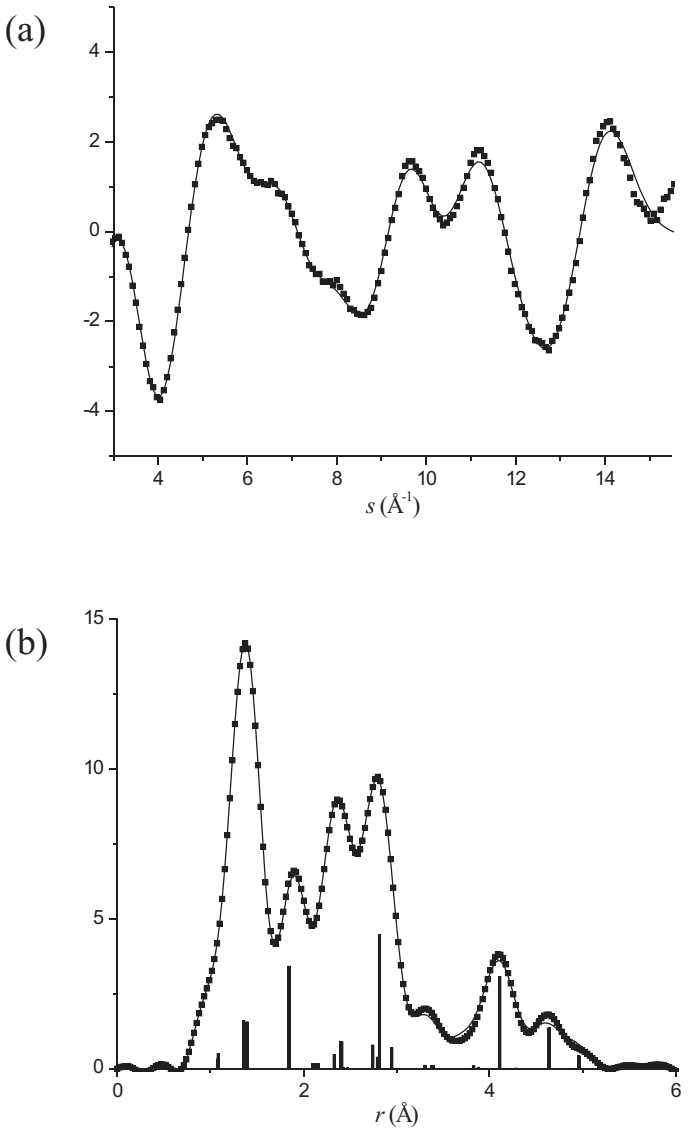

Fig. 5-4. The final refined theory (line) with experimental data (filled squares) for bromobenzene in (a) $sM(s)$ and (b) $f(r)$ representations. The fitted theory is quantified with ^{2} = 70.166 and R = 0.061. The vertical bars at each peak position have a height proportional to nZ_iZ_j/r.

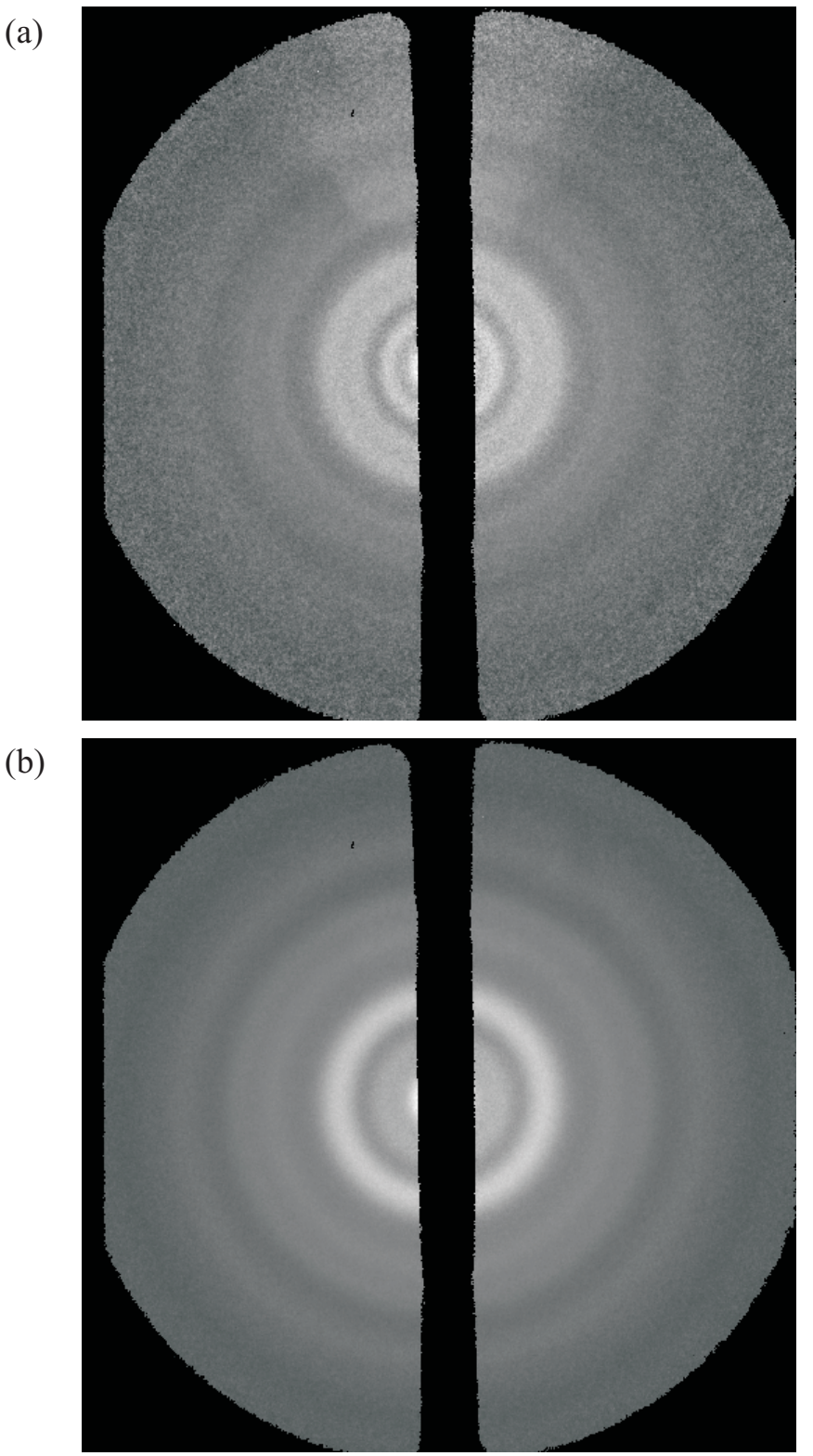

Fig. 5-5. The ratio patterns from diffraction by (a) iodobenzene and (b) 2-fluoropyridine.

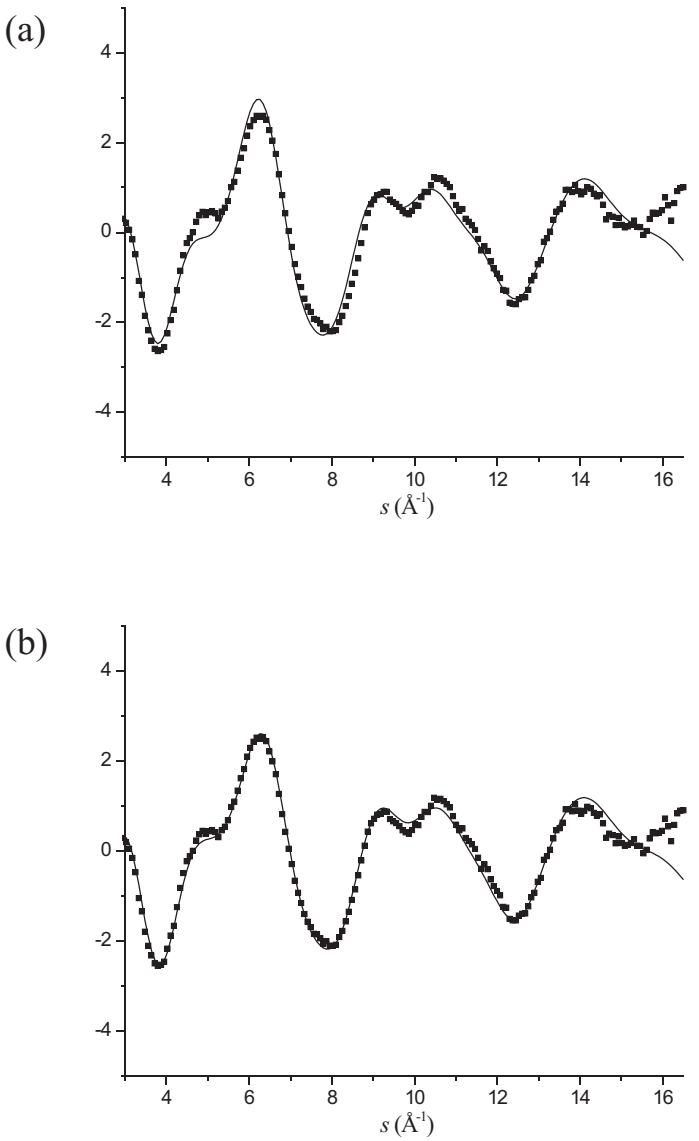

Fig. 5-6. *sM*(*s*) curves for iodobenzene showing theory (line) with experimental data (filled squares). The theoretical curve in (a) corresponds to that derived from the DFT structure (^{2} = 259.793; R = 0.173) and that in (b) is the DFT structure with a refined C-I bond distance (^{2} = 88.392; R = 0.102).

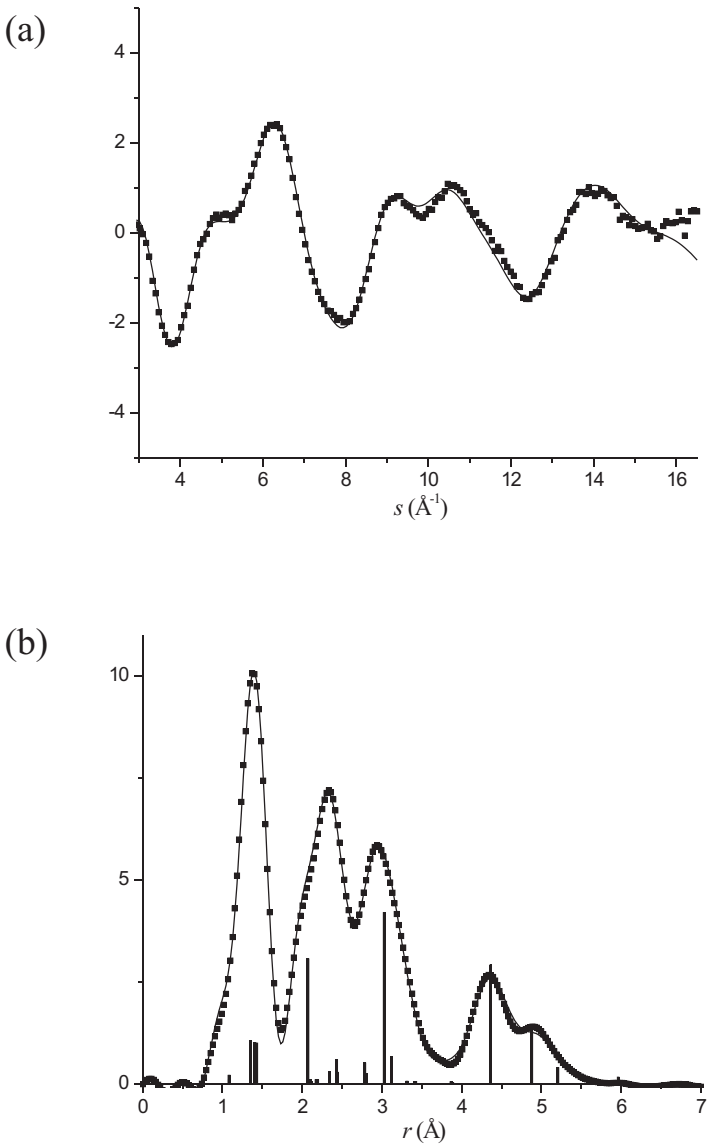

Fig. 5-7. The final refined theory (line) with experimental data (filled squares) for iodobenzene in (a) $sM(s)$ and (b) $f(r)$ representations. The fitted theory is quantified with $^2 = 69.192$ and $R = 0.089$. The vertical bars at each peak position have a height proportional to nZ_iZ_j/r.

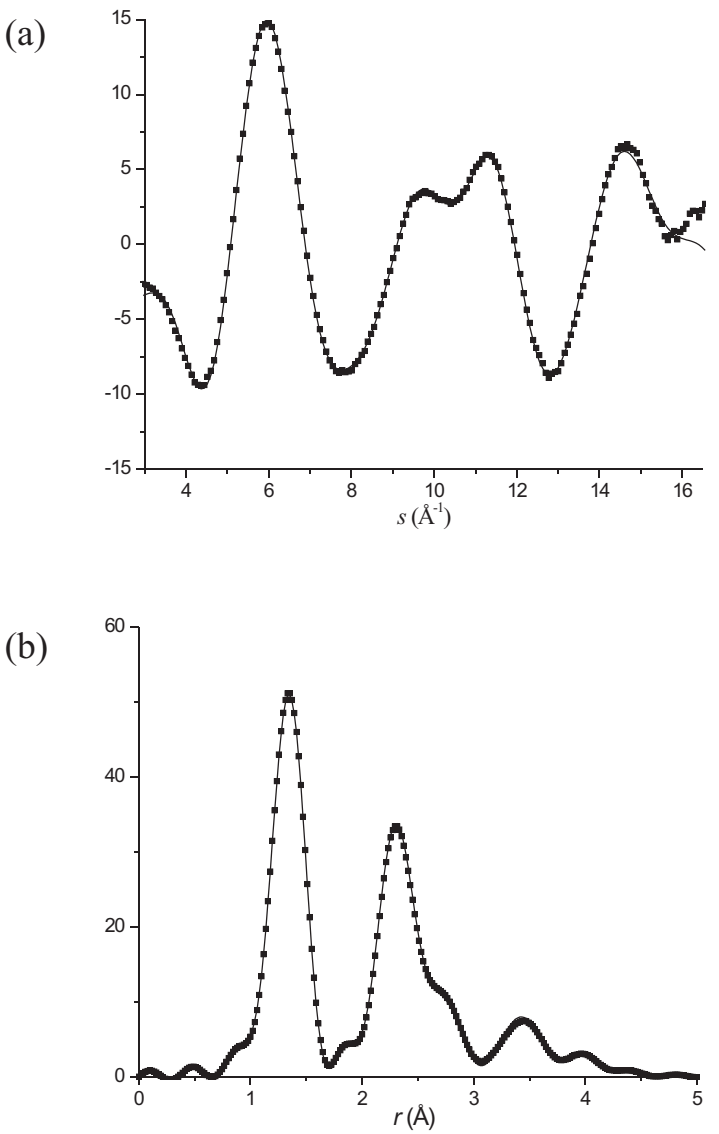

Fig. 5-8. The final refined theory (line) with experimental data (filled squares) for 2-fluoropyridine in (a) $sM(s)$ and (b) $f(r)$ representations. The fitted theory is quantified with $^2 = 89.686$ and $R = 0.035$.

(a)

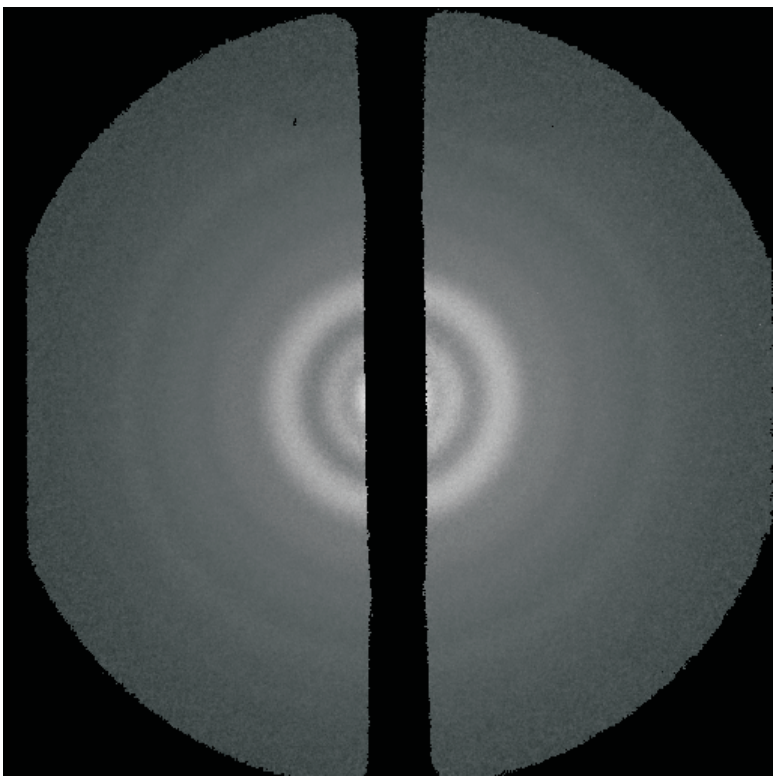

(b)

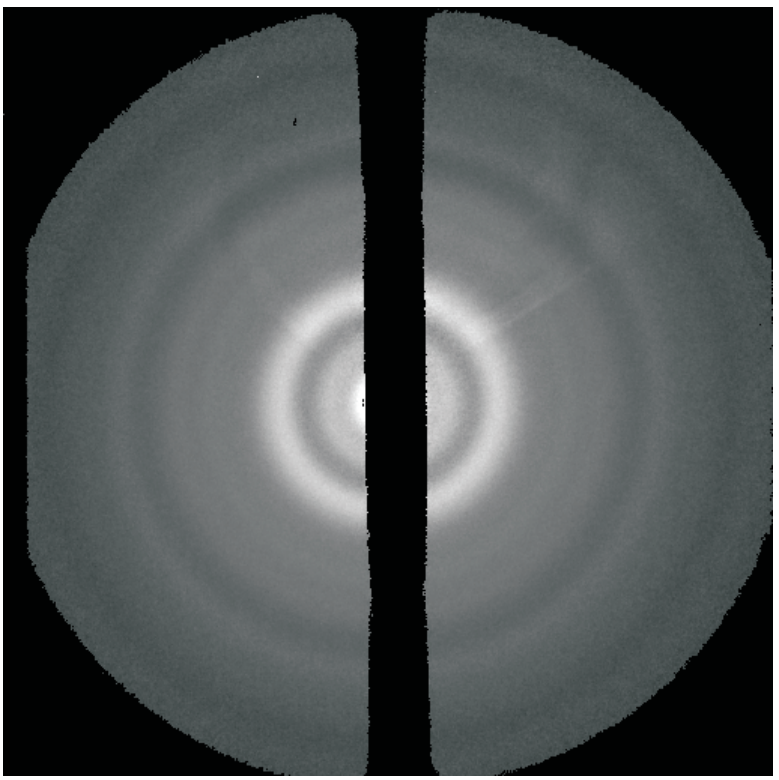

Fig. 5-9. The ratio patterns from diffraction by (a) acetylacetone and (b) benzaldehyde.

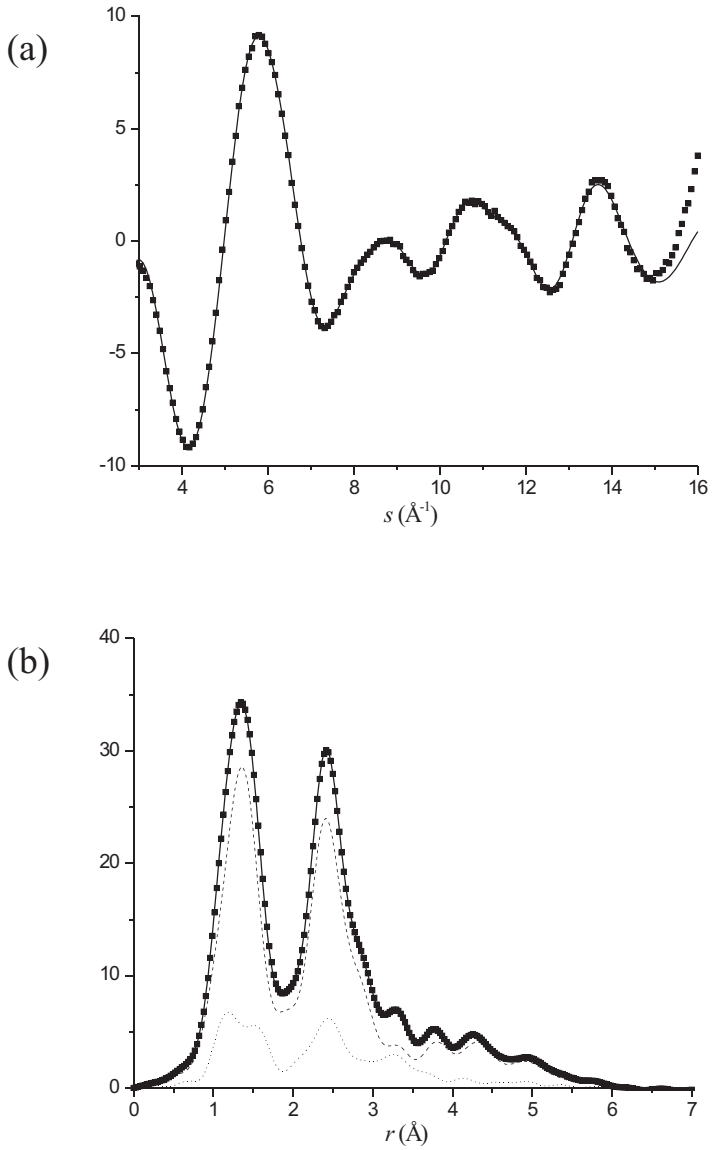

Fig. 5-10. The final refined theory (line) with experimental data (filled squares) for acetylacetone in (a) $sM(s)$ and (b) $f(r)$ representations. The fitted theory is quantified with $^2 = 41.676$ and $R = 0.030$. The $f(r)$ is broken up to show individual contribution from both enol (dashed) and keto (dotted) tautomers.

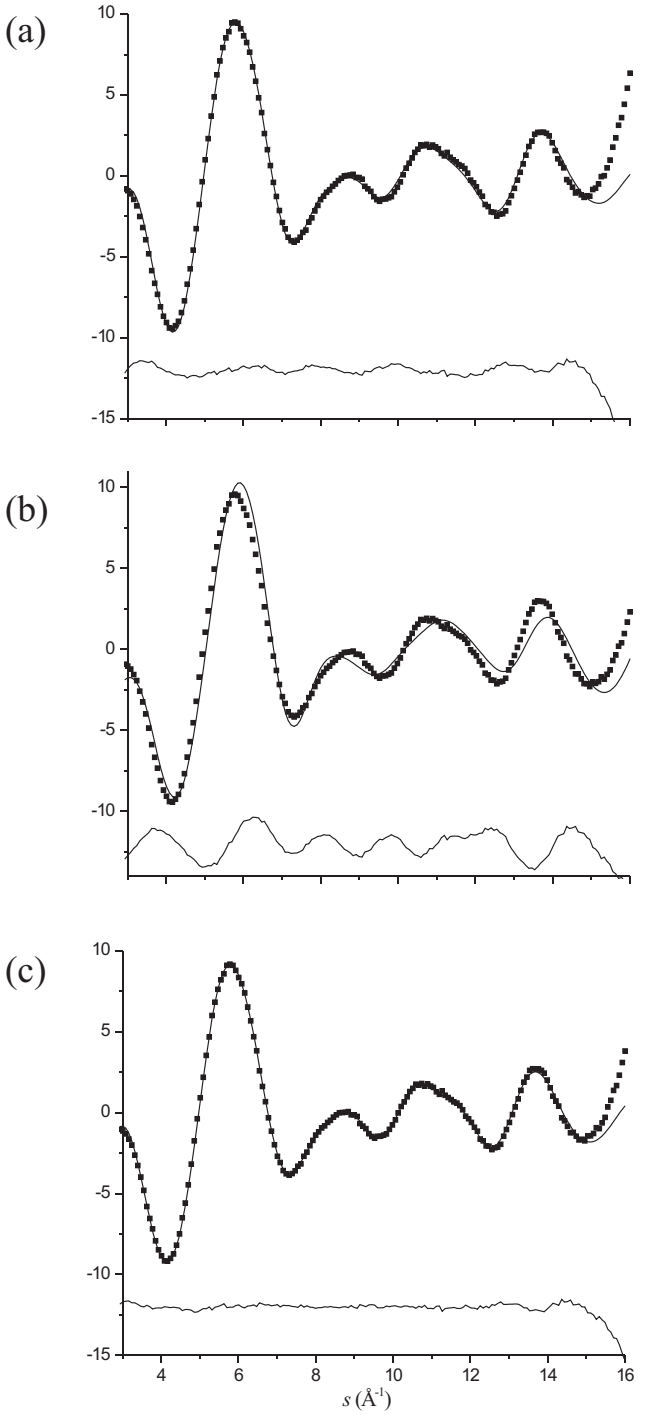

Fig. 5-11. *sM*(*s*) curves for various models with refined component fractional contributions. (a) 86% DFT C_s enol + 14% DFT keto tautomer; ^{2} = 198.320; R = 0.066. (b) 67% DFT C_{2v} enol + 33% DFT keto tautomer; ^{2} = 1423.836; R = 0174. (c) 78% refined C_s enol + 22% refined keto tautomer; ^{2} = 41.676; R = 0.030. The solid line below each plot is the residual (theory – experiment).

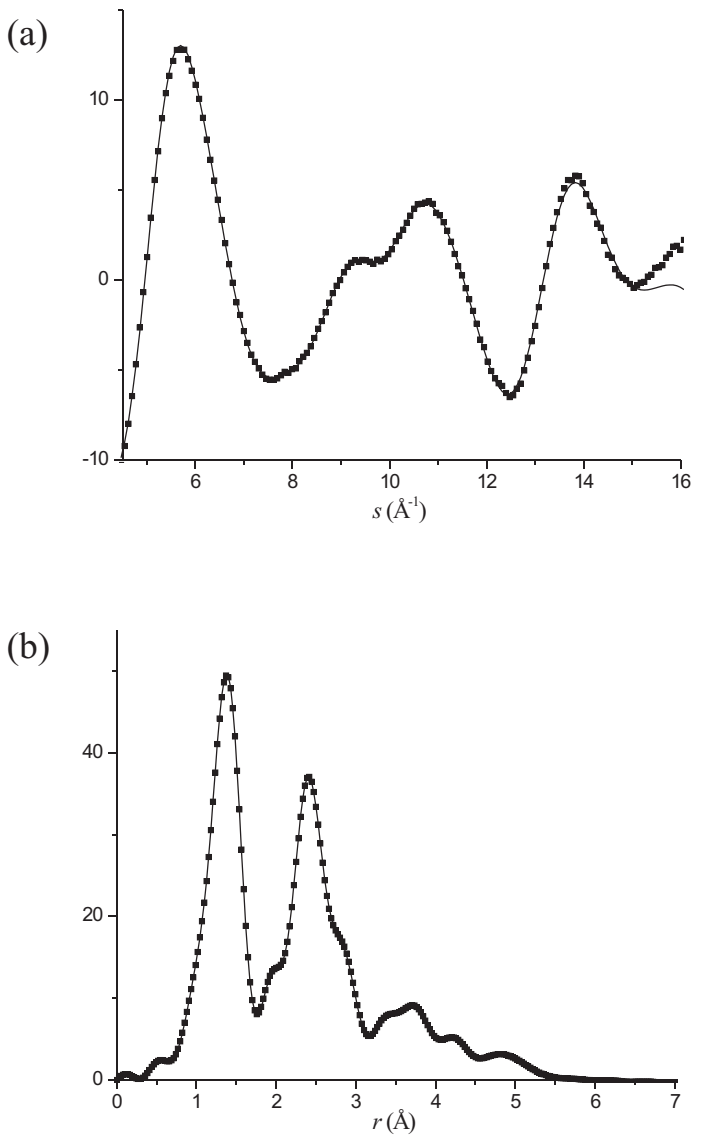

Fig. 5-12. The final refined theory (line) with experimental data (filled squares) for benzaldehyde in (a) $sM(s)$ and (b) $f(r)$ representations. The fitted theory is quantified with $^2 = 67.127$ and $R = 0.043$.

(a)

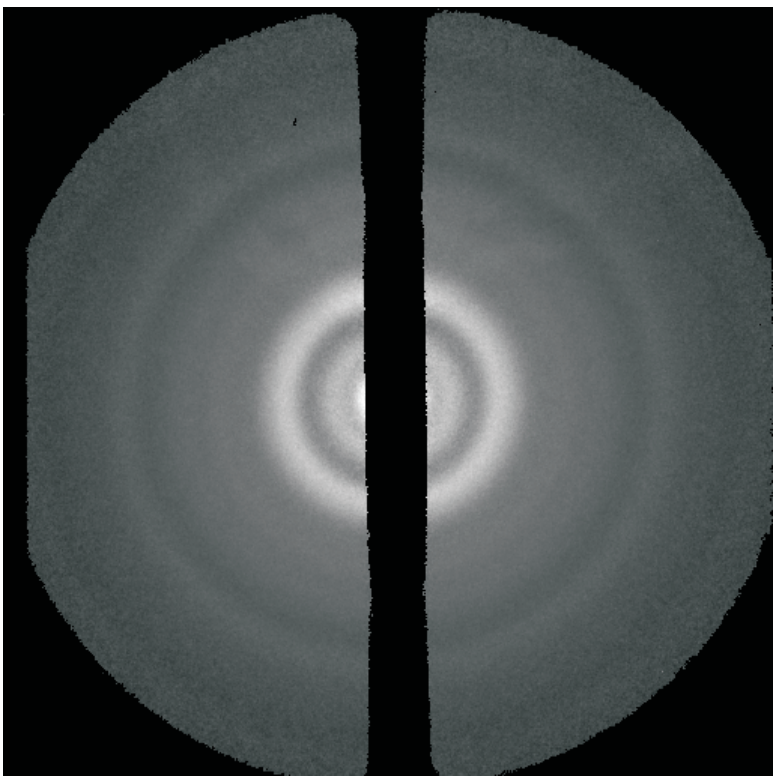

(b)

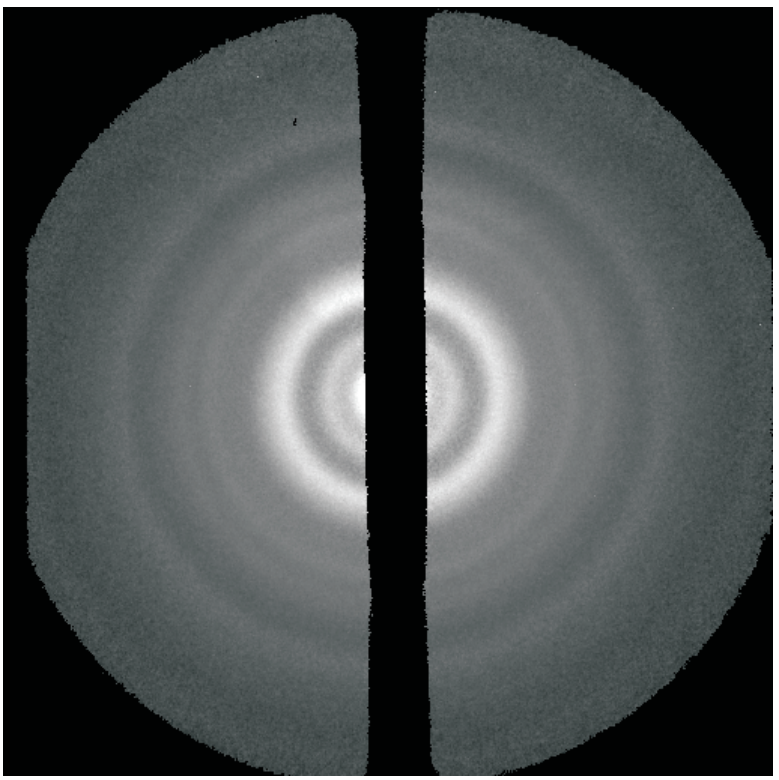

Fig. 5-13. The ratio patterns from diffraction by (a) acetophenone and (b) methylbenzoate.

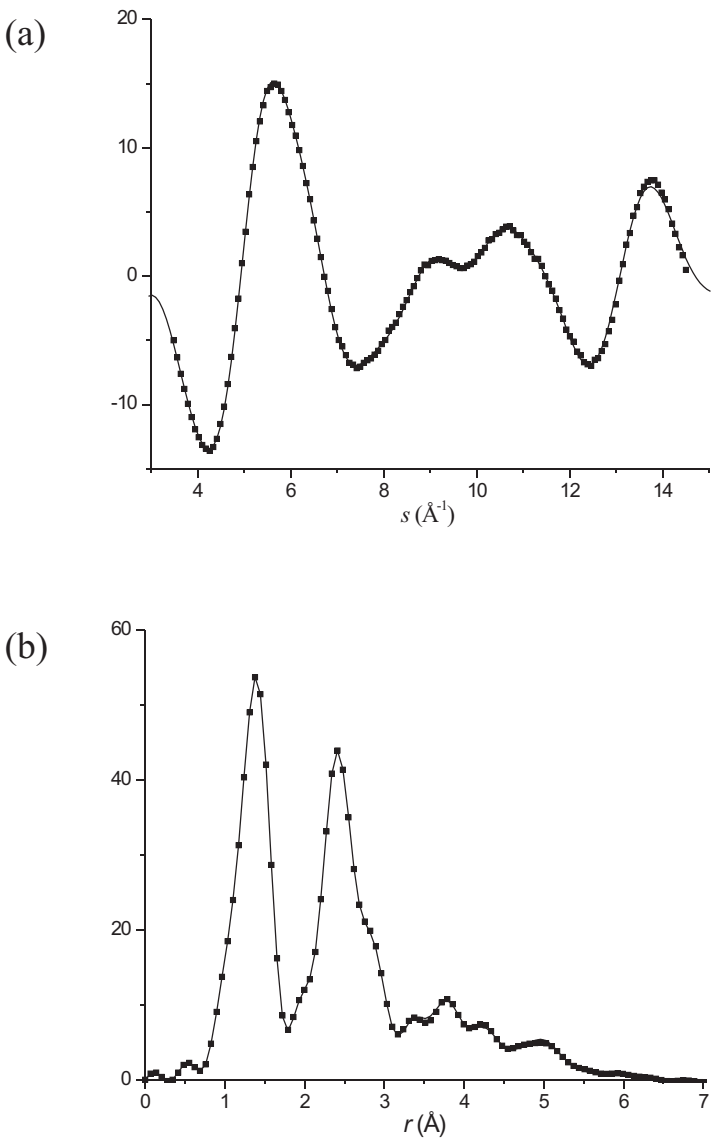

Fig. 5-14. The final refined theory (line) with experimental data (filled squares) for acetophenone in (a) $sM(s)$ and (b) $f(r)$ representations. The fitted theory is quantified with $^2 = 39.069$ and $R = 0.028$.

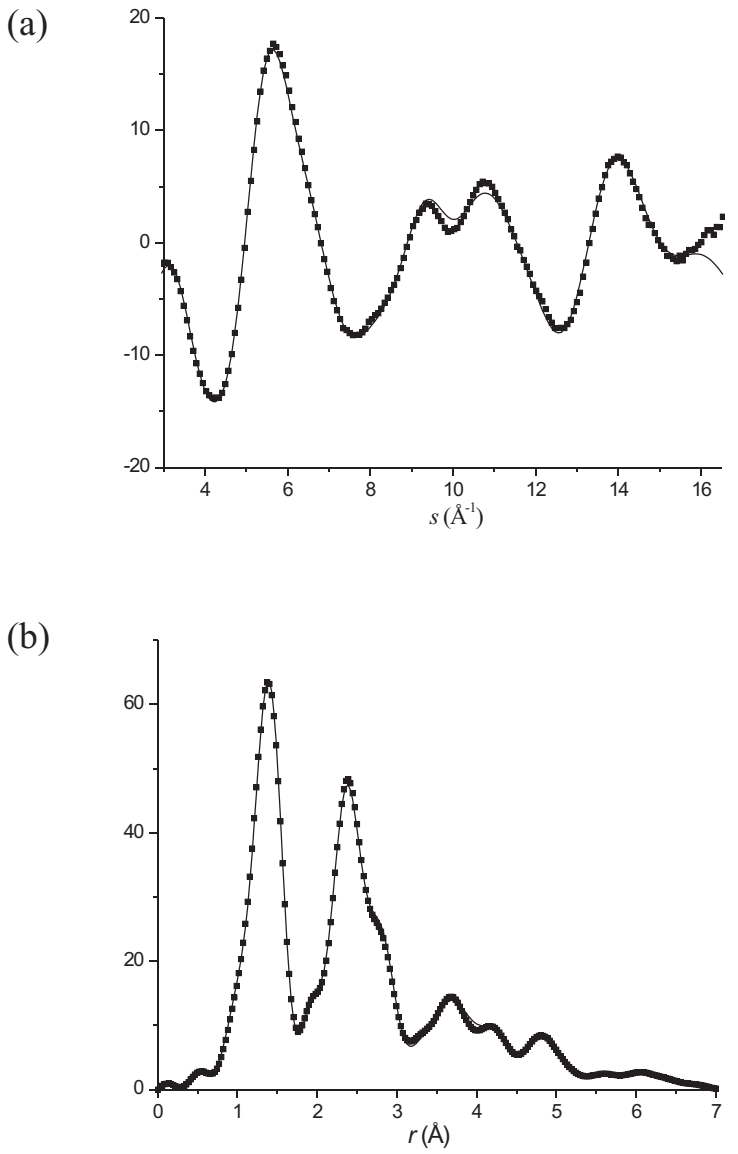

Fig. 5-15. The final refined theory (line) with experimental data (filled squares) for methylbenzoate in (a) $sM(s)$ and (b) $f(r)$ representations. The fitted theory is quantified with $^2 = 224.746$ and an $R = 0.056$.